Comparison of straggling functions calculated with Bethe-Fano, FVP and Rutherford cross sections

Hans Bichsel

November 13, 2011

e-mail: hbichsel@uw.edu Elossf-11NK.tex [Si-fano-alli;BFVP-Feb]

Center for Experimental Nuclear Physics and Astrophysics

Box 354290 University of Washington

Seattle, WA 98195-4290

Abstract

Energy loss distribution (or straggling) functions for the analysis of the ionization observed in particle detectors (TPC, SVT etc) must be calculated accurately (target: 1%). For thin absorbers (less than 300μm of Si or 10 cm for gases) Bohr or Vavilov calculations are not adequate. Instead a convolution or Monte Carlo method is needed. For all methods *differential collision cross sections (DCCS)* are needed. A brief description of the convolution method is given in the Introduction. Calculations with Bethe-Fano (B-F), Fermi-Virtual-Photon (FVP) and Rutherford approximations for DCCS are compared. Differences in the straggling functions caused by the differences in DCCS are described. At some places results of Vavilov calculations will also be shown.
A comparison between B-F convolutions and GEANT4 calculations will be given in another paper.

1 Introduction

Energy loss (or straggling) functions $P(\Delta)$, where Δ is the energy loss along a track segment of length x [1], can be calculated efficiently and accurately with a convolution method [2, 3, 4, 5]. [1] The *straggling function* for Δ is given by [6, 7, 8]

$$P(\Delta) = f(\Delta; x, v) \;=\; \sum_{n=0}^{\infty} P(n)\; \sigma(\Delta; v)^{*n} \tag{1}$$

where $P(n)$ is a *Poisson distribution* [2, 4, 5, 9] giving the probability density for n collisions in x

$$P(n) \;=\; \frac{m_c^n e^{-m_c}}{n!} \tag{2}$$

with $m_c = x \cdot M_0(v)$ the average number of collisions in x.

[1] Much detail not included here can be found in [2, 5]. Elastic scattering of the particles is not considered here.

The *straggling function* for *energy losses* in n collisions is $\sigma(\Delta;v)^{*n}$. It is the $n-$fold convolution of $\sigma(E;v)$, defined by

$$\sigma(\Delta;v)^{*n} = \int_0^{\Delta} \sigma(E;v) \cdot \sigma^{*(n-1)}(\Delta - E;v)\, dE, \quad \sigma(\Delta;v)^{*0} = \delta(\Delta), \quad \sigma(\Delta;v)^{*1} = \sigma(\Delta;v). \tag{3}$$

where $\sigma(E;v)$ is the collision cross section differential in energy loss E for single collisions of particles with speed v. Examples of $\sigma(\Delta;v)^{*n}$ are given in Figs. 11 and 12 of [7], and in [2, 4]. The convolution ("folding") method has also been used for calculations of multiple scattering [10].

2 Calculation of differential collision cross sections DCCS

For present purposes the Rutherford DCCS can be written as [5]

$$\sigma_R(E,\beta) \;=\; \frac{k}{\beta^2}\,(1-\beta^2\frac{E}{E_M})\;/\;E^2, \qquad k = 0.1535\; z^2\frac{Z}{A}\;\mathrm{MeVcm}^2 \tag{4}$$

where $\beta = v/c$ is the particle speed, E the energy loss in a collision, z the charge number of the incident particle, Z the atomic number and A the atomic mass in g/mol of the absorber..

The calculation of the Bethe-Fano (BF) differential collision cross section, DCCS [11, 12] and explicit equations are given in [6, 8], for Si is described in [6, 7, 8], for the Fermi-Virtual-Photon equations (FVP) in [6, 7]. Frequently the latter is called the PAI method. The DCCS for Si are compared in Fig. 1.

The cause of the difference between BF and FVP is given by the approximation shown in Fig. 2: in FVP the generalized oscillator strength GOS is approximated by a δ function.

The major purpose of this study is to present the differences of 10 to 20% in the results of energy loss calculations with BF and FVP DCCS. The differences between BF and Rutherford-Vavilov calculations can be much larger as shown in some of the figures.

At present I am not aware of any *program* calculating BF DCCS for gases. Therefore the calculations presented here give a comparison of straggling functions $f(\Delta)$ for Si calculated with B-F and FVP. *We can assume that gases will show similar trends,* see Tables 5-7.

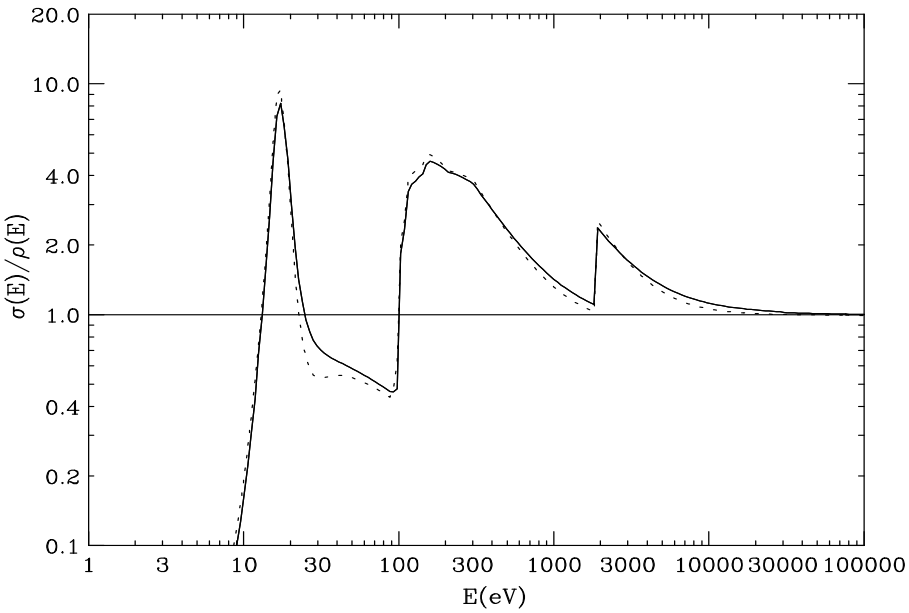

Figure 1: Inelastic collision cross sections $\sigma(E, v)$ for single collisions in silicon of minimum ionizing particles ($\beta\gamma = 4$), calculated with different theories. In order to show the structure of the functions clearly, the ordinate is $\sigma(E)/\sigma_R(E)$. The abscissa is the energy loss E in a single collision. The Rutherford cross section Eq. (4) is represented by the horizontal line at 1.0. The solid line was obtained with the Bethe-Fano theory, [8]. The cross section calculated with FVP [6, 7] is shown by the dotted line. The functions all extend to $E_M \sim 16$ MeV, see Eq. (6). The moments are $M_0 = 4$ collisions/μm and $M_1 = 386$ eV/μm, except $M_0 = 4000$ for the Rutherford DCCS with a nominal values $E_m \sim 0.005$ eV, Eq. (7).

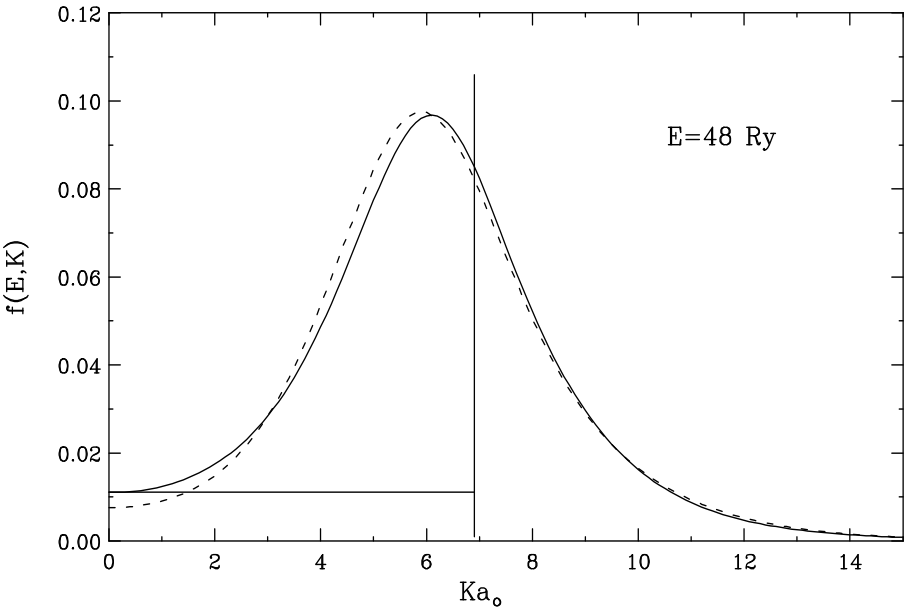

Figure 2: Generalized oscillator strength GOS for Si for an energy transfer $E = 650$ eV to the 2p-shell electrons [8]. Solid line: calculated with Herman-Skilman potential [13], dashed line: hydrogenic approximation [14]. The horizontal and vertical line define the GOS approximation used in FVP.

3 Moments M_ν of DCCS

In many discussions of energy loss functions attempts are made to derive their properties from the *moments of the* DCCS which are defined by

$$M_\nu(\beta) \;=\; \int E^\nu \; \sigma(E;\beta)\; dE \tag{5}$$

where $\beta = v/c$ is the particle speed, $\sigma(E;\beta)$ the DCCS [7, 15] and E the energy loss in a collision. It is customary to call M_1 the stopping power, and M_0 the total CCS. Comparisons of M_0 and M_1 for Si, Ne and Ar calculated for B-F and FVP are given in Appendix A.

We see that the values of the *stopping power* M_1 calculated with the two methods differ by less than 1%, while they differ by up to 15% for M_0. Since M_0 is a primary parameter in Eqs. 1 to 3 while M_1 does not appear, we must expect that effects on the straggling functions cannot be readily assessed from the values of M_1.

4 A qualitative estimate of the shape of the straggling functions

From Eq. (2) we see that the peak of the Poisson distribution will be proportional to M_0 and we can assume a width of the function $P(n)$ roughly proportional to $1/\sqrt{n}$. This will be the same for any absorber thickness x. The convoluted single collision spectra of Eq.(3) are complex, see Figs. 11 and 12 in [7] or 2.18 and 2.19 in [6]. We can conclude that there is no simple way to relate the properties of the *straggling functions* with the moments of Eqs.(2) and (3). As seen in Figs. 3 and 4 from the location of $< \Delta >$ the stopping power M_1 is not especially relevant for the description of the functions.

5 Comparisons of BF and FVP straggling functions.

Calculations of straggling functions with Eq. 1 were made with the B-F and FVP DCCS [2] for charged particles with speed $\beta\gamma = 0.316$ and 3.16, traversing Si layers with a thickness $x(\mu\text{m})$ along a *particle track*. Some of the functions are shown in Figs. 3 to 5, with comments in the captions. From the figures we see that the two factors in Eq. (1) have varied influence and importance in Figs. 3 and 4: the

[2] A comparison of the B-F and Rutherford DCCS is given by the Vavilov functions [5, 8] shown in some of the figures.

Poisson distribution appears for small energy losses and then disappears in the broader distribution produced by Eq. (3). [3] In Tables 1 to 4 values are given for two quantities related to Figs. 3-6: the most probable energy loss Δ_p and the FWHM w of $P(\Delta)$. Differences between BF and FVP results are given in percent. We see that the BF and FVP functions are similar in shape, but there is *no simple* dependence on x for the differences.

The *average number of collisions* along the track in x is given by $m_c = x\ M_0$ (below Eq. 2) and the *mean energy loss* is $< \Delta >= x\ M_1$. Values of M_0 and M_1 for Si are given in Table 5. For Tables 1 and 2 they are $M_0(0.316) = 30.3/\mu$m and $M_1 = 2.444$ keV/μm.

Note that Δ_p/x depends strongly on x and has little relation to $< \Delta > /x = M_1 = 2.44$ keV/mum (also see Table 8 in Appendix B).

Table 1: Comparison of Δ_p/x (keV/μm) and their ratio for B-F and FVP [7], Si, $\beta\gamma = 0.316$.

$x(\mu)$	$\Delta_p/x(BF)$	$\Delta_p/x(FVP)$	$diff\%$
0.33	0.4751	0.5113	7.6
0.66	1.0562	1.1320	7.2
1.25	1.2533	1.3166	5.1
2.5	1.4135	1.4645	3.6
10.0	1.7306	1.7731	2.4
50.0	2.0545	2.0778	1.1

Table 2: Comparison of w/x(kev/μm), their ratio and w/Δ_p [7], Si, $\beta\gamma = 0.316$.

$x(\mu)$	$w/x(BF)$	$w/x(FVP)$	$dif\%$	$w/\Delta_p(BF)$	$w/\Delta_p(FVP)$
0.33	1.5115	1.6485	9.1	3.181	3.224
0.66	1.4441	1.4558	0.8	1.367	1.286
1.25	1.2533	1.2298	−1.9	1.000	0.934
2.5	1.1071	1.0977	−0.8	0.783	0.750
5	1.0598	1.0318	0.97	0.675	0.638
10	0.9800	0.9605	0.98	0.566	0.541
50	0.8568	0.8187	−4.7	0.417	0.394

I have not found any usefull relation between $w(x)$ and x, see Figs. G.1 and G.2 in [7], also see Appendix B.

[3] Note that these features have been observed in energy loss measurements for very thin absorbers [5, 16].

Table 3: Comparison of Δ_p/x (eV/μm) and their ratio for B-F and FVP [7], Si, $\beta\gamma = 3.16$.

$x(\mu)$	$\Delta_p/x(BF)$	$\Delta_p/x(FVP)$	$diff\%$
2.5	119.2	121.8	2.2
5.0	151.7	159.0	4.8
10.0	178.0	184.1	3.4
20.0	196.8	201.8	2.5
40.0	216.4	221.1	2.2

Table 4: Comparison of w/x (eV/μm), their ratio and w/Δ_p [7], Si, $\beta\gamma = 3.16$.

$x(\mu)$	$w/x(BF)$	$w/x(FVP)$	$dif\%$	$w/\Delta_p(BF)$	$w/\Delta_p(FVP)$
2.5	232.1	235.8	1.6	1.947	1.937
5	200.2	201.2	0.5	1.320	1.266
10	162.9	162.6	−0.2	0.915	0.883
20	144.9	143.3	−1.1	0.736	0.710
40	137.6	135.5	−1.5	0.636	0.613

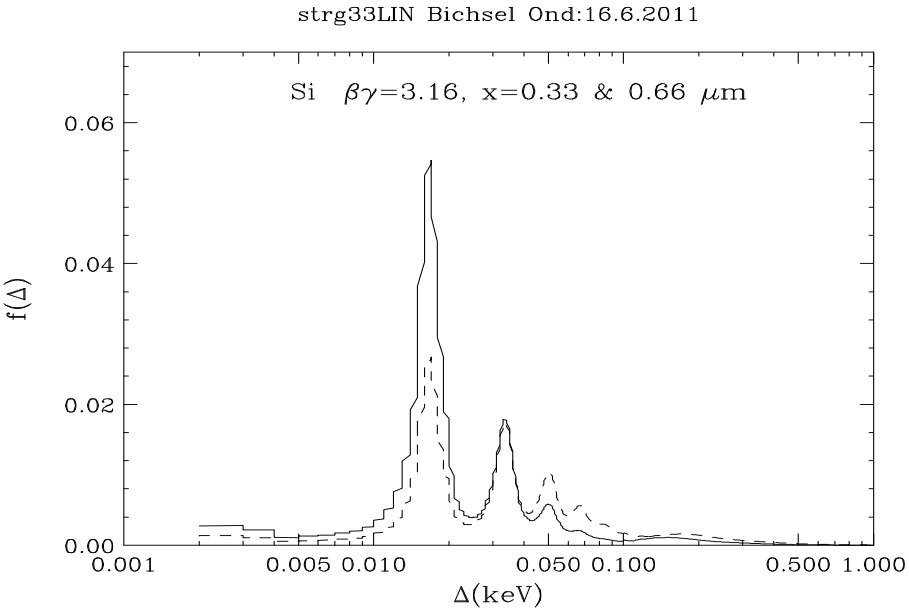

Figure 3: Straggling functions calculated with FVP method for particles with speed $\beta\gamma = 3.16$ traversing $x = 0.33$ μm (solid line, $m_c = 1.3$) and $x = 0.66$ μm (dashed line, $m_c = 2.6$) [16, 17]. Clearly neither the most probable values nor the FWHM have much meaning. We can see that the individual peaks approximate the Poisson distribution, but the increasing spread of $\sigma(\Delta; v)^{*n}$ reduces the Poisson peaks [5]. The mean value of the *energy loss* for $f(\Delta)$ is $< \Delta > (0.33) \sim 0.13$ keV, $< \Delta > (0.66) \sim 0.26$ keV.

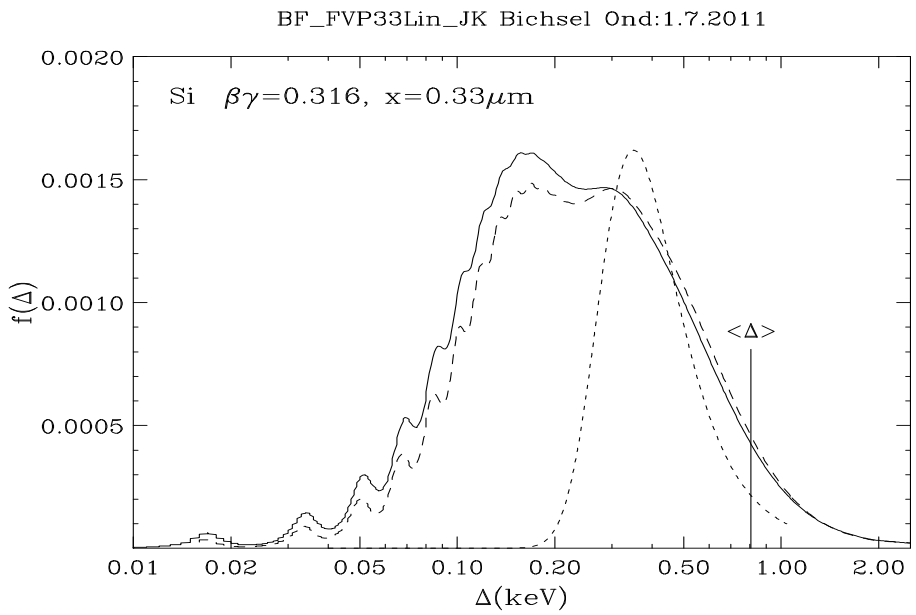

Figure 4: Straggling functions for particles with speed $\beta\gamma = 0.316$ traversing $x = 0.33$ μm. [8]. Solid line: calculated with BF, dashed line: FVP. Neither the most probable values nor the FWHM can be clearly defined. The Vavilov [18, 19] function is given by the dotted line. The mean energy loss is $< \Delta >$.

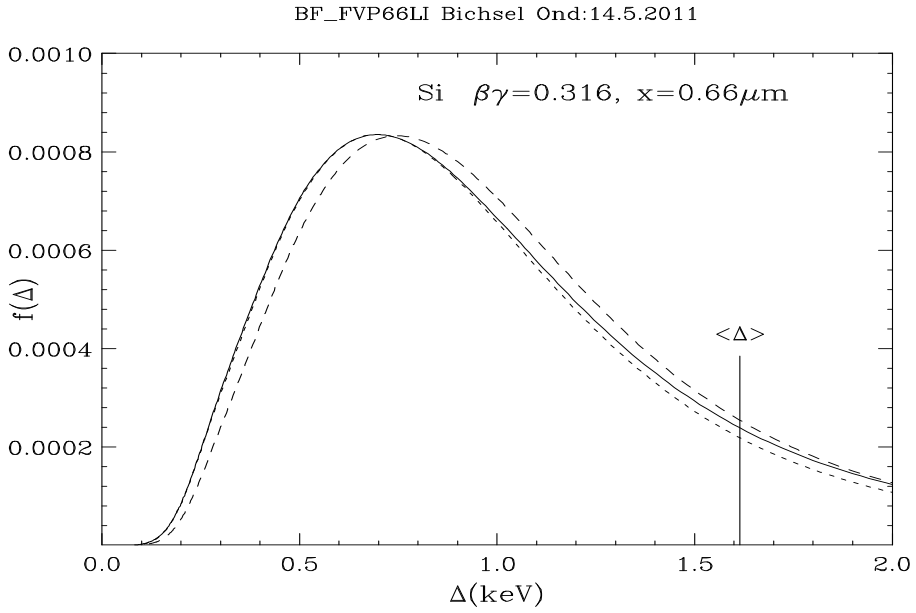

Figure 5: Straggling functions for particles with speed $\beta\gamma = 0.316$ traversing $x = 0.66$ μm. [8]. Solid line: calculated with BF $\Delta_p = 697$eV, $w = 953$eV, dashed line: FVP, $\Delta_p = 747$eV, $w = 961$eV. The ratio of the Δ_p is close to the ratio of the M_0 (Table 5), while that of the w is close to that of M_1. The dotted line: FVP for $x = 0.626\mu$m, chosen to obtain $\Delta_p = 697$eV, and $w = 924$eV. The reader is encouraged to contemplate these effects.

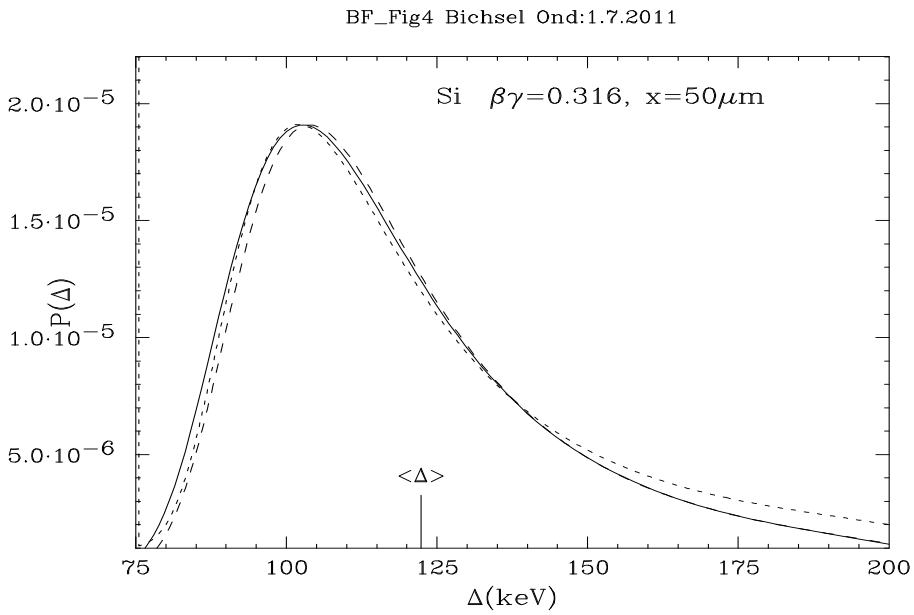

Figure 6: Straggling functions for particles with speed $\beta\gamma = 0.316$ traversing $x = 50$ μm. [8]. The functions have been normalized to the same value at the peak. Solid line: calculated with BF, dashed line: FVP. The most probable values are $\Delta_p(BF) = 102.7$ keV and $\Delta_p(FVP) = 103.9$ keV, differing by 1.1%, much less than the difference in M_0 seen in Table 5. The FWHM differ by 4.7%. The dotted line represents the Vavilov function with $\Delta_p(Vav) = 102$ keV and FWHM 10% smaller.

6 Conclusions

The results presented in Sect. 5 are much more complex than the differences between F-B and FVP shown in the Tables in Appendix A. I am not aware of any analytic approach which would give the results shown in Figs 3-6 and in Tables 1-4. Calculations with the complete DCCS for both B-F and FVP for high energy tracks have been made only for Si to my knowledge. [4]

From the results in Sect. 5 it is evident that the parameter M_0 is much more important than the stopping power M_1. For an accurate determination of M_0 the full DCCS must be available, in particular the generalized oscillator strength (GOS) [11, 12]. The FVP (or PAI) approximation gives fairly large differences shown in Appendix A.

Therefore I suggest that the Bethe-Fano method should be used for detectors of high energy particles, and that the Bethe-Fano DCCS should calculated.

[4] I have no *practical* knowledge about the methods used for electrons [20].

A Comparison of the *moments* calculated with B-F and FVP

The program to calculate the DCCS $\sigma(E;\beta)$ for Si with the B-F method was developed early [8] and used to generate the straggling functions. Results agreed well with experimental data. Later I modified the program to calculate these functions for Si, Ar and Ne with FVP [7].

Comparisons of the moments M_0 and M_1 for Si are given in Table 5.

Table 5: Comparison of M_0 (coll/μm) and M_1 (eV/μm) for B-F and FVP for Si.

	M_0			M_1		
bg	$B-F$	FVP	$diff\%$	$B-F$	FVP	$diff\%$
0.316	30.32	32.78	8.1	2443.7	2465.3	0.9
1.000	6.729	7.175	6.6	578.3	581.8	0.6
3.981	3.952	4.189	6.0	386.1	387.9	0.5
10.000	3.842	4.068	5.9	416.9	418.6	0.4
100.000	3.842	4.066	5.8	503.8	505.4	0.3

Studies of the Bethe-Fano DCCS were made by Saxon [21, 22, 23, 24], but only the functions for the moments are currently available. The differences for M_1 are also less than 1%, same as for Si. Calculations of M_0 functions were made for protons with kinetic energy T with this method [6, 8, 7] and are compared with the FVP functions in Tables 6 and 7. For practical reasons the coefficient k/β^2 of Eq.(4) is not used, and thus the Bethe-Lindhard function L for the collision cross section M_0 is given in the tables.

Table 6: Comparison of L for protons traversing Ar calculated with FVP, Eq.(7) of [7], and Eq.(1) in [23] (using $\mathcal{J}_1 - \mathcal{J}_2 = 4.268$).

T(MeV)	L_F	L_B	$diff\%$
10	13.59	11.89	14.3
30	15.65	13.93	12.3
100	17.81	16.06	11.1
300	19.69	17.87	10.2
500	20.58	18.73	9.9
1000	21.95	20.05	9.5
3000	24.76	22.81	8.5
10000	28.66	26.70	7.3
30000	32.57	30.67	6.2

Table 7: Comparison of L for Ne calculated with FVP and with Eq.(2) [7], using $\mathcal{J}_1 - \mathcal{J}_2 = 4.268$.

T(MeV)	L_F	L_B	$diff\%$
10	34.56	31.02	11.4
30	39.37	35.82	9.9
100	44.40	40.85	8.7
300	48.68	45.13	7.9
500	50.70	47.15	7.5
1000	53.81	50.26	7.1
3000	60.31	56.77	6.2
10000	69.40	65.96	5.2
30000	78.01	75.30	3.6

The difference in M_0 is quite large for accurate work and should be explored further, especially for gases. We see that a similar difference in M_0 occurs for Si, Ne and Ar. The stopping power M_1 calculated with FVP differs by less than 1% from the values given in ICRU 49.

B Asymptotic values of Δ_p for thick segments

In the historical studies of energy losses it is postulated that the *mean energy loss* for a straggling function is given by $< \Delta >= x \cdot M_1$. From Figs. 2-6 we see that the position of $< \Delta >$ is quite implausible while the most probable energy loss Δ_p is fairly well defined for $m_c > 20$, Fig. 5. I have made calculations for Δ_p for a range of $\beta\gamma$ and x and give Δ_p/x in Table 8. We see that Δ_p/x approaches the value of M_1 only for particle speeds below "minimum ionization". [5]

[5]The programs used for this study will be posted at [15]

Table 8: Values of Δ_p/x(MeV/cm) as a function of segment thickness t for several particle energies T.

$T =$	14	6.6	2.93	1.16	0.39 GeV
$\beta\gamma =$	16	8	4	2	1
$M_1 =$	4.37	4.07	3.85	4.05	5.77
$x(cm)$			$\Delta_p/x\ MeV/cm$		
0.0078	2.41	2.34	2.31	2.55	3.94
0.0625	2.81	2.74	2.72	3.32	4.67
0.125	2.93	2.86	2.85	3.32	4.90
0.25	3.04	2.98	2.97	3.32	5.12
0.5	3.16	3.10	3.10	3.47	5.33
1	3.28	3.22	3.22	3.61	5.52
2	3.41	3.34	3.35	3.74	5.65
4	3.51	3.45	3.46	3.84	5.71
8	3.56	3.50	3.50	3.89	–

C Convolution with the Rutherford DCCS

It is interesting to compare the Laplace transform method [5, 18, 19] with the convolution method: just use the DCCS of Eq.(4), with the limits used by Landau [18]

$$E_M \ = \ 2mc^2\ \beta^2\ \gamma^2 \tag{6}$$

where m is the electron mass and

$$E_m \ = \ \frac{I^2}{E_M} \cdot \exp(\beta^2) \tag{7}$$

in order to get a good approximation for the stopping power M_1. [6] An example is given in Fig. 7. A slight displacement is related to the difference in the energy loss scales: for the convolutions a logarithmic scale is used, for the Laplace calculations a linear one. We can see that the *numerical* programs for Laplace and convolution calculations give close agreement for $f(\Delta)$.

[6] With this value of E_m the number of collisons per unit track length, M_0, will be very large.

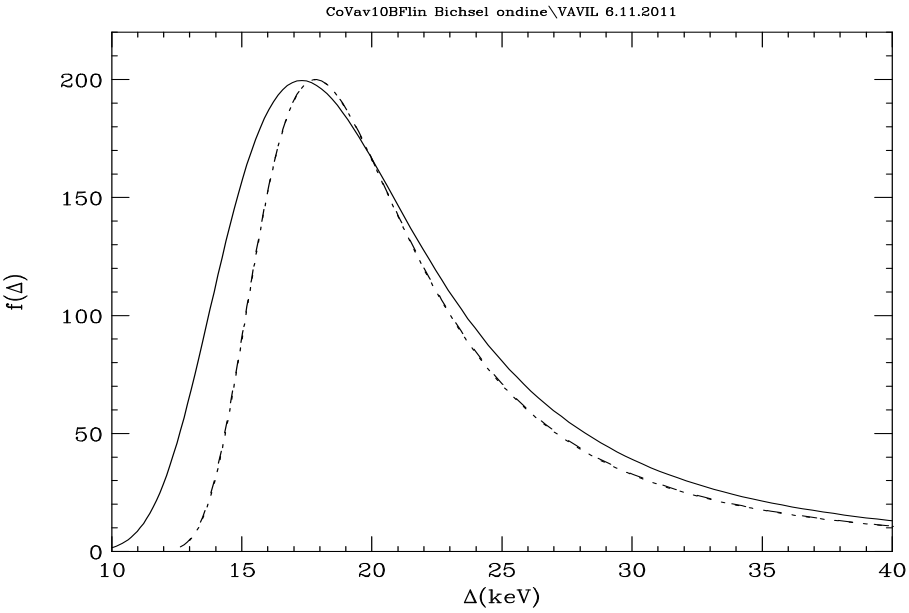

Figure 7: Straggling functions for protons with speed $\beta\gamma = 0.316$ traversing $x = 10$ μm of Si. dotted line: Vavilov method: Laplace transforms, DCCS of Eq.(4), dashed line: convolution method, DCCS of Eq.(4), $m_c \sim 6800$, Eq.(2). The two functions overlap closely: the most probable values are $\Delta_p(BF) = 17.79$ keV and $\Delta_p(FVP) = 17.83$ keV, differing by 0.2%. The FWHM $w \sim 7.8$ keV differ by 0.4%. The function calculated with the convolution method and the Bethe-Fano DCCS (shown in Fig. 1) is given by the solid line, $\Delta_p(BF) = 17.3$ keV, $w = 9.8$ keV and $m_c = 303$. For other comparisons see [5, 8].

References

[1] H. Bichsel, *A method to improve tracking and particle identification in TPCs and silicon detectors*, Nucl. Instr. Meth. B **52** (1990) 136-139

[2] E. J. Williams, The Straggling of β-Particles, Proc. Roy. Soc. A **125** (1929) 420.

[3] Herring, J. R., and E. Merzbacher, 1957, J. Elisha Mitchell Sci. Soc. @73, 267.

[4] Kellerer, A. M., 1968, G. S. F. Bericht B-1, Strahlenbiologisches Institut der Universität München.

[5] H. Bichsel, R. P. Saxon, Comparison of calculational methods for straggling in thin absorbers, Phys. Rev. **A 11** (1975) 1286.

[6] H. Bichsel, *Interaction of radiation with matter*, in Landolt-Boernstein, New Series, Group I, Vol.21, Elementary Particles, Subvolume B, Detectors for Particles and Radiation, H. Schopper and C. Fabjan Eds., Springer (2011).

[7] *A method to improve tracking and particle identification in TPCs and silicon detectors,* Hans Bichsel, Nucl. Instr. and Meth. **A 562** (2006) 154-197.

[8] H. Bichsel, Rev. Mod. Phys. **60** (1988) 663. The doubling method used was described by A. Kellerer [4].

[9] R. D. Evans, The Atomic Nucleus, eleventh printing, McGraw Hill, N. Y. (1967).

[10] *Multiple scatt,* "Multiple scattering correction for proton ranges and the evaluation of the L-shell correction and I-value for Al" Bichsel, H. and E. A. Uehling (1960), Phys. Rev. **119** (1960) 1670.

[11] *Penetration of protons, alpha particles and mesons.* H. Bethe,

[12] *Penetration of protons, alpha particles and mesons.* U. Fano, Ann. Rev. Nucl Sci. **13** (1963) 1-66.

[13] Manson, ST. (1972). Inelastic collisions of fast charged particles with atoms: ionization of the aluminum L shell, Phys. Rev. **A 6**, 1013-1024.

[14] Walske, M.C. *The stopping power of K-electrons*, Phys. Rev. **88** (1952) 1283-1289, and *Stopping power of L-electrons*, Phys. Rev. **101** (1956) 940-944.

[15] *Inelastic collision cross sections, convolutions etc* will be posted at website: http://faculty.washington.edu/hbichsel/

[16] J. Ph. Perez, J. Sevely, and B Jouffrey, Phys. Rev. **A 16** (1977) 1061.

[17] *Energy spectra of electron yields from silicon: Theory and experiment"*, Z. Chaoui, Z.J. Ding, K. Goto, Phys. Lett A **373** (2009) 1679

[18] *On the energy loss of fast particles by ionization* L. Landau, [Sov.] J. Phys. **VIII** (1944) 201.

[19] *Ionization Losses of High-Energy Heavy Particles* . P. V. Vavilov, Soviet Physics JETP **5** (1957) 749

[20] F. Salvat (Barcelona) private communication, 2011.

[21] M Inokuti and Y-K Kim and R L Platzman Phys Rev **164** (1967) 55

[22] Inokuti, M. (1971). *Inelastic collisions of fast charged particles with atoms and molecules- the Bethe theory revisited.* Rev. Mod. Phys. **43**, 297-347, and **50**, 23 (1978).

[23] R. P. Saxon, Phys. Rev. A **8** (1973) 839.

[24] M Inokuti, R P Saxon and J. L. Dehmer, Int J Radiat Phys Chem **7** (1975) 109